Journal of Wood Science

NOTE

Open Access

Evaluation method for embedment stiffness of metal washers in bolted timber joints using torque gradient and nut factor

Doppo Matsubara[1*], Masaki Teranishi[2] and Takuro Mori[3]

Abstract

Assessing the residual performance of timber joints affected by decay is important for seismic diagnosis and reinforcement of timber structures. This study introduces a method to evaluate the embedment stiffness of metal washers in bolted timber joints using a torque wrench. Formulas for the embedment stiffness of metal washers using the torque gradient (the gradient of the tightening torque against the tightening rotation angle of the nut) and the nut factor are presented and the calculated values are compared with experimental values obtained by conducting tightening tests with a torque wrench and embedment tests of metal washers in bolted joints made from Japanese cedar, Hiba, and Japanese cypress. The results show that the experimental values of the embedment stiffness of metal washers in Japanese cedar and Hiba are generally within the range of the values calculated from the minimum and maximum values of the nut factor. However, for Japanese cypress, the values calculated from the maximum value of the nut factor exceed the experimental values. This was presumably due to locally large frictional forces generated on the bearing surface or threaded part.

Keywords Bolted timber joints, Embedment stiffness, Torque gradient, Tightening torque, Nut factor

Introduction

Wood is easily affected by moisture and, especially in high-humidity environments, wood-rot fungus can lead to biological deterioration, resulting in a significant decrease in strength, etc. [1–6]. Wooden buildings with deteriorated members are likely to exhibit reduced structural performance, so, to ensure structural safety, it is necessary to replace or reinforce the deteriorated members. Particularly in the case of wooden structures, the performance of joints often dictates the overall performance of the structure. Therefore, when planning the reinforcement, it is necessary to assess the residual strength and stiffness in the joints affected by decay. Thus far, research has focused on the survival performance of joints affected by wood decay, including nail joints [7–12], screw joints [13–16], and bolt/drift pin joints [17]. Many of these studies evaluated the relationship between decay and joint shear performance.

In contrast, the present study focuses on bolted connections, which are the most common connection type in wooden structures. There are two forms of resistance mechanisms, where either tensile force or shear force is applied to the bolt [18]. For the tensile force case, joint performance is dominated by the embedment of metal washers, whereas the shear force case involves the bending yield. For this, when the diameter length ratio (main material thickness/bolt diameter) is large and the bending deformation of the bolt increases, the shear resistance increases because of the bolt's axial tensile force, resulting in the so-called rope effect becoming significant. In

*Correspondence:
Doppo Matsubara
d.matsubara@fuk.kindai.ac.jp
[1] Kindai University, 11-6 Kayanomori, Iizuka, Fukuoka 820-8555, Japan
[2] Niigata University, 8050, Ikarashi 2-no-cho, Nishi-ku, Niigata 950-2181, Japan
[3] Hiroshima University, 1-4-1, Kagamiyama, Higashihiroshima, Hiroshima 739-8527, Japan

this situation, an embedment force is generated on metal washer that balances the bolt's tensile force, and the rope effect becomes more pronounced as embedment stiffness of the metal washer increases [19].

Therefore, embedment of metal washers is one of the governing factors for the strength performance of bolted joints and a comprehensive understanding of the embedment behavior of metal washers is crucial. For example, wooden houses with poor underfloor ventilation or which have not been treated with preservatives are at risk of wood rot and this results in reduced performance of the anchor joints. Therefore, a method to comprehend and evaluate the residual performance of the embedment of metal washers is essential. Therefore, this study aimed to establish a method to accurately evaluate the residual performance of bolted joints affected by wood decay and present a method to directly measure and evaluate the embedment stiffness of metal washers on-site. It first focused on the relationship between bolt tightening torque, axial force, and nut rotation angle. It theoretically demonstrated that the embedment stiffness of metal washers can be calculated by combining these relationships and derived a formula for theoretical calculations. Bolt joint tightening tests were conducted using a torque wrench and embedment tests of metal washers were performed using Japanese cedar, Hiba, and Japanese cypress of different densities and the agreement between the calculated and the experimental values was examined.

Theory

This study examined the bolted timber joint shown in Fig. 1. It consists of a stud bolt, metal washer, nut, timber member, and steel plate (rigid body). The derivation of the following equations is based on the work of Fukuoka et al. [20].

First, the relationship between tightening torque T_f and clamping force F_b when the nut is tightened is expressed as:

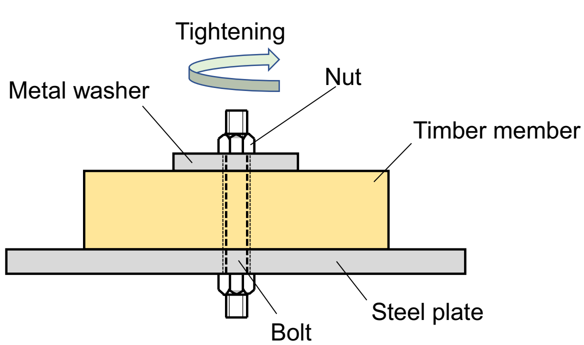

Fig. 1 Bolted timber joints

$$T_f = K_n F_b d, \tag{1}$$

where K_n is the nut factor and d is the bolt diameter. Here, K_n can also be expressed using Eq. (2) below [21]:

$$K_n = \frac{1}{d}\left(\frac{P}{2\pi} + 0.577\mu_{th} d_2 + 0.5\mu_b D_b\right), \tag{2}$$

where μ_{th} is the coefficient of friction between threads, d_2 is the effective thread diameter, μ_b is the coefficient of friction between bearing surfaces and D_b is the equivalent frictional diameter on the bearing surface. The terms inside parentheses in Eq. (2) show the breakdown of torque consumption: the first term is the torque expended on clamping force of thread pitch's inclined plane, the second term is the torque expended on thread friction, and the third term is the torque expended on bearing surface friction [22]. Therefore, K_n is highly dependent on the friction between the bearing surface and the threaded part.

Furthermore, if the steel plate is regarded as a rigid body, the rotation angle φ when the bolt is tightened is expressed as [23]:

$$\varphi = \frac{360}{P}\left(\frac{1}{K_b} + \frac{1}{K_{ew}}\right)F_b, \tag{3}$$

where K_{ew} is the embedment stiffness of the metal washer, K_b is the stiffness of the bolt, P is the thread pitch. Here, K_b can be calculated as a series combination of the spring constants K_{th}, K_s, and K_{cyl} for thread engagement, thread play, and bolt cylinder, respectively, using the following equation:

$$\frac{1}{K_b} = \left(\frac{2}{K_{th}} + \frac{2}{K_s} + \frac{1}{K_{cyl}}\right), \tag{4}$$

where K_{th}, K_s, and K_{cyl} can be calculated as follows:

$$K_{th} = \frac{A_s E_b}{L_{th}}, \tag{5}$$

$$K_s = \frac{A_s E_b}{L_s}, \tag{6}$$

$$K_{cyl} = \frac{A E_b}{L_{cyl}}, \tag{7}$$

where A_s is the effective cross-sectional area of the thread; A is the cross-sectional area of the cylinder; E_b is Young's modulus, which is set to 205,000 N/mm^2 here; L_s is the thread play length; L_{cyl} is the length of the cylindrical part of the bolt (See Fig. 2); and L_{th} is equivalent

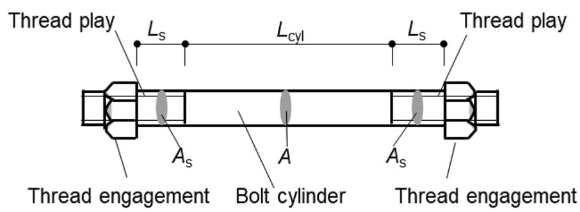

Fig.2 Bolt details

length, which can be calculated using the bolt's nominal diameter d as follows [24]:

$$L_{\mathrm{th}} = 0.85d \tag{8}$$

Equation (1) can be solved for F_{b}, substituted into Eq. (3), and rearranged for K_{ew} as follows:

$$K_{\mathrm{ew}} = \frac{360}{P\left\{K_{\mathrm{n}}d - \frac{360}{P}\left(\frac{1}{K_{\mathrm{b}}}\right)\left(\frac{T_{\mathrm{f}}}{\varphi}\right)\right\}}\left(\frac{T_{\mathrm{f}}}{\varphi}\right) \tag{9}$$

Therefore, from Eq. (9), if the torque gradient T_{f}/ϕ, which is the gradient of the tightening torque with respect to rotation angle, and the nut factor K_{n} are known, then the embedment stiffness of the metal washer, K_{ew}, can be calculated.

Materials and methods

Materials

Japanese cedar (*Cryptomeria japonica*), Hiba (*Thujopsis dolabrata*), and Japanese cypress (*Chamaecyparis obtusa*) wood specimens with dimensions of 105 mm (T: Tangential direction) × 140 mm (L: Longitudinal direction) × 30 mm (R: Radial direction) and with a ϕ 13 mm bolt hole in the center were used. Fifteen specimens of each species were prepared and six specimens of each species were used in each experiment to investigate the embedment yield load of metal washer P_{y} and the embedment stiffness of metal washers K_{ew} and the torque gradient T_{f}/ϕ. The densities and moisture content of the specimens, presented as the mean ± standard deviation, were 314 ± 4 kg/m^3, 9.5 ± 0.7% for Japanese cedar, 401 ± 4 kg/m^3, 12.2 ± 0.9% for Hiba, and 504 ± 9 kg/m^3, 13.1 ± 0.3% for Japanese cypress. M12 stud bolts made of S45C material, with a thread pitch P of 1.75 mm, thread length of 38 mm, cylindrical length L_{cyL} of 24 mm, and a total length of 100 mm. The nut was a hexagonal nut of S45C material, with a bilateral width of 18.6 mm and a height of 10 mm. The washer was 42 mm in diameter and 3.2 mm thickness, and made from SWCH with a ϕ 13 mm bolt hole in the center.

Embedment test for measuring P_y

Figure 3 shows the experimental apparatus. The specimen was placed on a steel component and loaded monotonically in the R direction up to a displacement of 3 mm using a universal testing machine (AG-Xplus 50 kN, Shimadzu Corp.). Displacement was defined as the travel of the crosshead. The test speed was 2 mm/min. From the obtained load–displacement relationship, the linear slope in the elastic range and the secondary slope in the plastic range were calculated using the least-squares method and the intersection point of the two lines was designated as P_{y} [25].

Tightening test for measuring nut factor K_n

Figure 4 shows the experimental apparatus. To investigate the nut factor K_{n}, a bolt tightening test was conducted using a tightening test machine (NST-500Nm, Japan Measuring System Co.). Each material was placed in the testing machine, the nut was tightened, and the tightening torque of nut and clamping force was measured with a load cell. The clamping force was limited to 10 kN. Five tightening speeds (0.5, 1, 4, 10, and 20 rpm) were utilized,

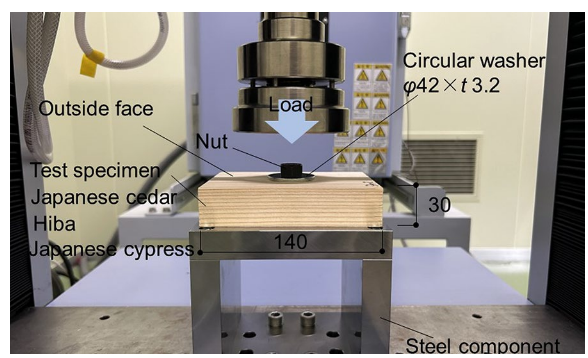

Fig. 3 Embedment test of a metal washer for measuring P_{y} (units: millimeters)

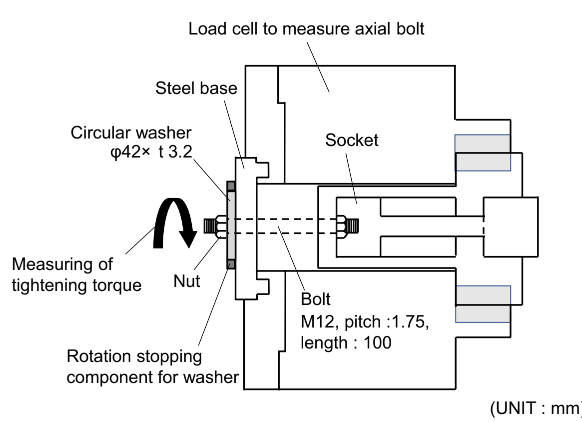

Fig. 4 Tightening test method for measuring nut factor

with six specimens for each condition. K_n was calculated from the relationship between the obtained tightening torque and clamping force at 5 kN using Eq. (1).

Tightening test for measuring T_f/φ and embedment test for measuring K_{ew}

Figure 5 shows the experimental apparatus. To obtain T_f/ϕ, the target tightening torque T_A was first determined as set out below.

The maximum tightening torque needed to obtain the target maximum clamping force F_{max} is T_{max}, the minimum tightening torque needed to obtain the target minimum clamping force F_{min} is T_{min}, and T_A is the average of these values:

$$T_{A} = \frac{(T_{max} + T_{min})}{2} \tag{10}$$

T_{max} and T_{min} are expressed based on Eq. (1) as, respectively:

$$T_{max} = K_{n-min} F_{max} d, \tag{11}$$

$$T_{min} = K_{n-max} F_{min} d, \tag{12}$$

where $K_{n\text{-}min}$ and $K_{n\text{-}max}$ are the minimum and maximum nut factors, respectively, using the minimum and maximum values obtained from the bolt tightening test using the tightening test machine as described above.

On the other hand, T_{max} and T_{min} have the following relationship when a torque wrench is used for the torque method. The error rate of torque for a torque wrench is m and the target tightening torque T_A must be less than T_{max} and more than T_{min}, taking into account the error of the torque wrench. T_{max} and T_{min} are expressed, respectively, as:

$$T_{A}\left(1 + \frac{m}{100}\right) \leq T_{max} \tag{13}$$

$$T_{A}\left(1 - \frac{m}{100}\right) \geq T_{min}, \tag{14}$$

where, since the equals sign holds when the upper and lower limits of T_A are reached, taking into account the error of the torque wrench. The F_{min} corresponding to T_{max} and T_{min} can be derived from Eqs. (11, 12, 13, 14), as:

$$F_{min} = \frac{K_{n-min}}{K_{n-max}} \frac{\left(1 - \frac{m}{100}\right)}{\left(1 + \frac{m}{100}\right)} F_{max} \tag{15}$$

In this study, F_{max} was set to 70% of the mean value of P_y for each species of tree. The error rate m was set at 1% [26].

Using a digital torque wrench (DPW-50-P, Adrec Corp.), which can measure the tightening torque and rotation angle in real time using dedicated software, the nut was slowly tightened and the tightening was stopped when T_A was reached. The tightening operation was performed while checking the tightening torque values monitored on the dedicated software. T_f/ϕ was then calculated from the relationship between the obtained tightening torque and the rotation angle.

Next, after investigating T_f/ϕ for each specimen, an embedment test of the metal washers was conducted to examine the embedment stiffness of the metal washer, K_{ew}. The experimental method was the same as for P_y

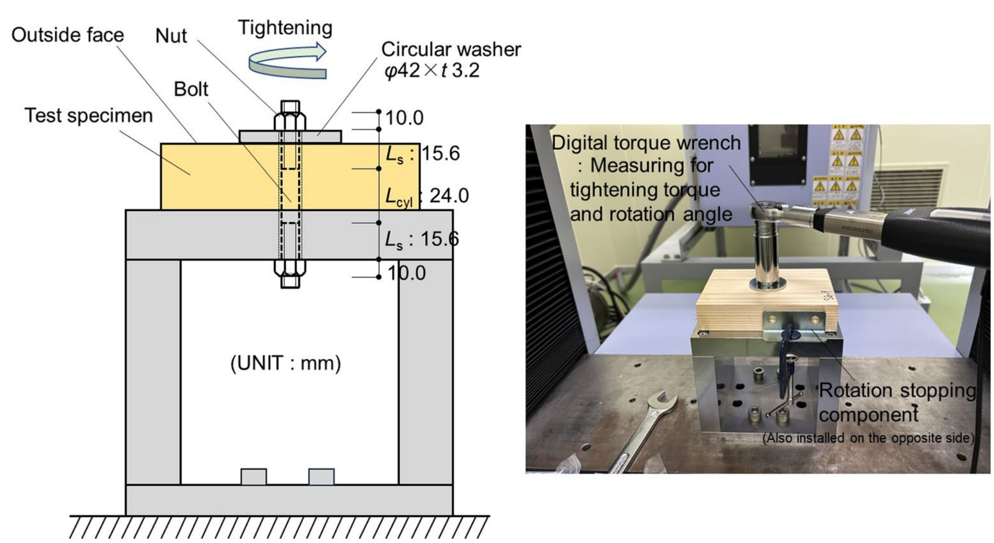

Fig. 5 Tightening test apparatus for measuring T_f/φ

above. Force was applied until F_{max} was reached and the linear slope was obtained from the load–displacement relationship by the least-squares method, and this was used as K_{ew}.

Results and discussion

Results of P_y and K_n

Figure 6 shows the average load–displacement relationship obtained from the embedment tests of metal washers (to experimentally determine P_y). It shows that, although the initial slip is slightly larger for Hiba, the load increases linearly, reaches a relatively clear yield point, and then tends to increase in a nonlinear manner. Based on this relationship, the linear slope in the elastic range (K_{ew}) was defined at load interval of 2–3 kN for Japanese cedar, 3–4 kN for Hiba, and 5–6 kN for Japanese cypress. The linear slope in the plastic range (K_{pw}) was defined as 1–3 mm displacement for all species. P_y was calculated as the intersection of both slopes by the least-squares method. The calculated characteristic values are listed in Table 1. The table also shows the determined F_{max} (=0.7×P_y). According to the results, K_{ew} and P_y were largest for Japanese cypress, followed by Hiba and then Japanese cedar.

Figure 7 shows the relationship between nut factor K_n and tightening speed obtained from the bolt tightening tests. According to this, at a tightening speed of 20 rpm, the variation in K_n was smaller than at other tightening speeds, but no clear relationship between tightening speed and K_n was observed. $K_{n\text{-}min}$ was 0.25 and $K_{n\text{-}max}$ was 0.37. This large variation in K_n under no-lubrication conditions has been reported in several previous studies [27, 28].

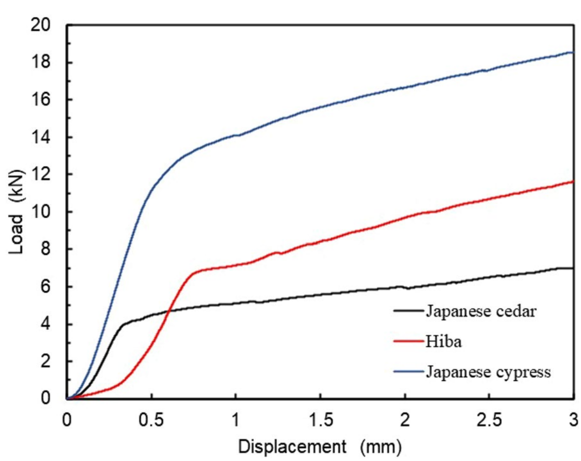

Fig. 6 Relationship between load and displacement obtained from the embedment test

Table 1 Characteristic values of each wood specimen

Specimen		K_{ew} [kN/mm]	K_{pw} [kN/mm]	P_y [kN]	F_{max} (=0.7×P_y) [kN]
Japanese cedar	Avg	18.1	1.01	4.36	3.05
	S.D	4.58	0.25	0.61	
Hiba	Avg	25.3	2.13	6.63	4.64
	S.D	0.62	0.42	0.73	
Japanese cypress	Avg	29.8	2.13	13.5	9.43
	S.D	1.53	0.11	0.67	

Avg.: Average, *S.D.*: Standard deviation, K_{pw}: Secondary embedment stiffness of washer into timber member

Comparison of calculated and experimental values

Table 2 shows T_A values calculated using the determined F_{max}, $K_{n\text{-}min}$, and $K_{n\text{-}max}$ values. Figure 8 shows a typical relationship between T_f and ϕ. As shown in the figure, for Hiba, a large ϕ value was required for T_f to increase linearly similarly to what was observed in Fig. 6. Based on the obtained results, the $T_A\times0.5 - T_A\times0.8$ Nm intervals for Japanese cedar, Hiba, and Japanese cypress were calculated using the least-squares method for T_f/ϕ.

Table 3 shows the $K_{ew\text{-}cal}$ values of each specimen calculated from Eq. (8) using these results, including $K_{ew\text{-}cal.1}$ and $K_{ew\text{-}cal.2}$ calculated from $K_{n\text{-}min}$ (=0.25) and $K_{n\text{-}max}$ (=0.37), in addition to $K_{ew\text{-}exp}$ calculated from the washer penetration experiment. Here, the same method used to calculate P_y was used to calculate $K_{ew\text{-}exp}$. As shown in Table 3, for all Japanese cedar and Hiba specimens, except one, $K_{ew\text{-}exp}$ was within the range of $K_{ew\text{-}cal.1}$ and $K_{ew\text{-}cal.2}$ calculated from $K_{n\text{-}min}$ and $K_{n\text{-}max}$. However, five out of the six Japanese cypress specimens had lower

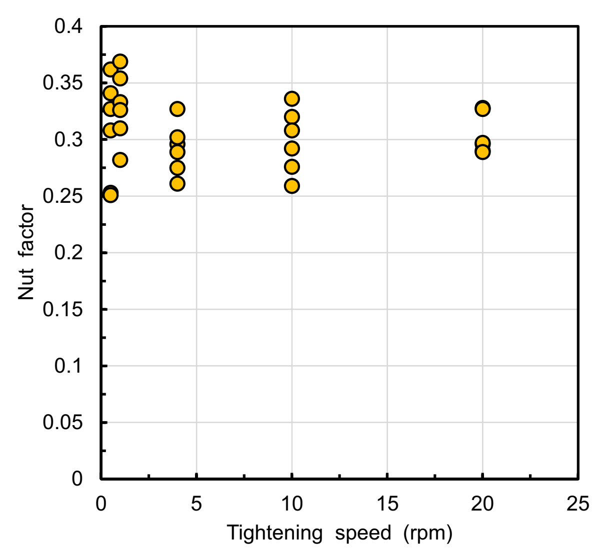

Fig. 7 Relationship between K_n and tightening speed

Table 2 Calculated values of T_A

Specimen	$K_{n\text{-min}}$	$K_{n\text{-max}}$	F_{min} [kN]	F_{max} [kN]	T_{min} [Nm]	T_{max} [Nm]	T_A [Nm]
Japanese cedar	0.25	0.37	2.04	3.05	9.0	9.2	9.1
Hiba			3.09	4.64	13.7	14.0	13.8
Japanese cypress			6.29	9.43	27.8	28.4	28.1

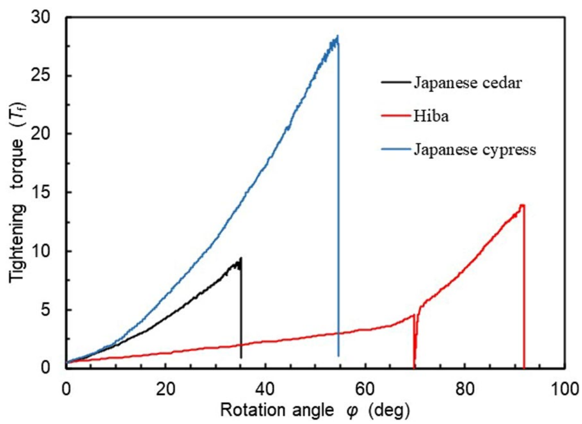

Fig. 8 Relationship between tightening torque and rotation angle

$K_{ew\text{-}exp}$ values than $K_{ew\text{-}cal.1}$ values calculated from $K_{n\text{-}max}$. A reason for $K_{ew\text{-}exp}$ being lower than $K_{ew\text{-}cal.1}$ calculated from $K_{n\text{-}max}$ may be that K_n was actually larger than $K_{n\text{-}max}$. In addition, Table 3 shows the results of $K_{n\text{-}cal}$ also calculated using Eq. (9). It can be seen that the specimens whose $K_{ew\text{-}exp}$ values are lower than the $K_{ew\text{-}cal.1}$ values calculated from $K_{n\text{-}max}$ are higher than the $K_{n\text{-}max}$ value of 0.37. Since the tightening work was performed using a manual torque wrench, it is assumed that, when tightening with a large tightening force, a large frictional force is generated locally on the bearing surface or at the thread, resulting in an increase in K_n.

From the above, $K_{ew\text{-}cal}$ was evaluated as being overestimate depending on the K_n setting and the species of wood. In future, the use of automatic tools may be explored, such as nut runners that allow tightening to occur at a constant speed, to stabilize the friction on the bearing surface or thread and prevent variations in K_n. Furthermore, in this study, lubricating oil was not applied to metal objects such as bolts. But by applying lubricating oil to the bearing surface and threads, friction against torque could be reduced and a more accurate K_{ew} value

Table 3 Comparison of calculated and experimental values

Specimen	Number	T_f/φ [Nm/deg]	$K_{ew\text{-}cal.1}$[a] [kN/mm]	$K_{ew\text{-}cal.2}$[b] [kN/mm]	$K_{ew\text{-}exp}$ [kN/mm]	$K_{n\text{-}cal}$
Japanese cedar	1	0.373	18.6	28.3	21.4	0.32
	2	0.393	19.7	30.1	21.2	0.34
	3	0.388	19.4	29.7	22.3	0.33
	4	0.368	18.3	27.9	22.0	0.31
	5	0.288	14.1	21.4	22.2	0.24
	6	0.308	15.2	23.0	18.4	0.31
Hiba	1	0.509	26.1	40.4	24.9	0.38
	2	0.351	17.4	26.5	25.1	0.26
	3	0.437	22.1	33.9	24.9	0.33
	4	0.440	22.3	34.2	25.1	0.33
	5	0.442	22.4	34.3	25.6	0.33
	6	0.431	21.8	33.4	25.1	0.32
Japanese cypress	1	0.577	30.0	46.8	30.4	0.36
	2	0.722	38.8	61.5	30.0	0.46
	3	0.820	45.0	72.2	33.4	0.48
	4	0.682	36.3	57.3	32.1	0.41
	5	0.684	36.4	57.5	32.5	0.41
	6	0.705	37.7	59.8	31.7	0.43

[a] Calculated value obtained from $K_{n\text{-}max}$ (=0.37)

[b] Calculated value obtained from $K_{n\text{-}min}$ (=0.25)

could be expected regardless of the type of tool used for tightening.

Conclusions

Formulas for the embedment stiffness of metal washers using torque gradient and nut factor were presented for bolted timber joints. Tightening and embedment tests of metal washers were conducted using a torque wrench on bolted joints made of three species of wood: Japanese cedar, Hiba, and Japanese cypress. The experimental values for Japanese cedar and Hiba were found to fall within the range of embedment stiffness values for metal washers calculated from the minimum and maximum nut factors in all but one of the six specimens. However, for five of the six Japanese cypress specimens, the calculated maximum nut factors exceeded the experimental values. This was presumably due to locally large frictional forces generated on the bearing surface or threaded part.

Acknowledgements
Not applicable.

Author contributions
DM designed and performed the experiments and analyzed the data. MT and TM analyzed the data. All authors read and approved the final manuscript.

Funding
This work was supported in part by the research Grant of the Maeda Engineering Foundation.

Availability of data and materials
Not applicable.

Declarations

Ethics approval and consent to participate
Not applicable.

Consent for publication
We agree to allow our manuscript being published.

Competing interests
The authors declare that they have no competing interests.

Received: 23 November 2023 Accepted: 17 January 2024
Published online: 29 January 2024

References

1. Kennedy R (1958) Strength retention in wood decayed to small weight losses. For Prod J 8:308–314
2. Brown F (1963) A tensile strength test for comparative evaluation of wood preservatives. For Prod J 13:405–412
3. Mizumoto S (1966) The effect of decay caused by *Gloeophyllum trabeum* on the strength properties of Japanese red pine sap-wood. J Jpn For Soc 48:7–11
4. Toole E (1971) Reduction in crushing strength and weight associated with decay by rot fungi. Wood Sci 3:172–178
5. Mori T, Yanase Y, Tanaka K, Kawano K, Noda Y, Mori M, Kurisaki H, Komatsu K (2013) Evaluation of compression and bending strength properties of wood damaged from bio-deterioration (in Japanese). J Soc Mater Sci Jpn 62:280–285
6. Takanashi R, Ishihara W, Sawata K, Sano Y, Azuma T, Mori M, Koizumi A, Sasaki Y, Hirai T (2014) Fractography of shear failure surface of softwood decayed by brown-rot fungus. J Wood Sci 60:186–193
7. Scott MK, Robert JL, David VR, Jefferey JM (2005) Effects of decay on the cyclic properties of nailed connections. J Mater Civ Eng 17(5):579–585
8. Toda M, Mori M, Ohashi Y, Hirai T (2010) Effects on wood decay on the shear performance of nailed timber joint (in Japanese). Mokuzai Gakkaishi 56(1):41–47
9. Mori T, Tanaka T, Kawano K, Nakahata T, Yanase Y, Kurisaki H (2014) Estimation of shear strength of nail driven into decayed wood of Japanese cedar Sugi (in Japanese). J Soc Mater Sci Jpn 63:314–319
10. Takanashi R, Sawata K, Sasaki Y, Koizumi A (2017) Withdrawal strength of nailed joints with decay degradation of wood and nail corrosion. J Wood Sci 63(2):192–198
11. Sawata K, Sasaki Y (2018) Lateral strength of nailed timber connections with decay. J Wood Sci 64:601–611
12. Ueda R, Sawata K, Sasaki T, Sasaki Y (2021) Effects of decay on the shear properties of nailed joints parallel and perpendicular to the grain. J Wood Sci. https://doi.org/10.1186/s10086-021-02006-1
13. Mori T, Noda Y, Azuma T, Mori M, Toda M (2014) Evaluation of single shear performance of wood screw joint after compulsive decay (in Japanese). Kouzou Kougaku Ronbunsyu 60B:371–375
14. Mori T, Noda Y, Azuma T, Mori M, Toda M, Ishida H (2015) Evaluation of single shear strength performance of wood screw joint driving into compulsive decayed wood (in Japanese). Kouzou Kougaku Ronbunsyu 61B:237–241
15. Takanashi R, Toda M, Miyauchi T, Mori M, Mori T (2018) Shear strength of multi-screw joints connected to decayed lumber (in Japanese). Mokuzai Gakkaishi 64(3):122–129
16. Ueda R, Sawata K, Takanashi R, Sasaki Y, Sasaki T (2020) Degradation of shear performance of screwed joints caused by wood decay. J Wood Sci. https://doi.org/10.1186/s10086-020-01889-w
17. Sawata K, Sasaki T, Doi S, Iijima Y (2008) Effect of decay on shear performance of dowel-type timber joints. J Wood Sci 54:356–361
18. Sawata K (2015) Strength of bolted timber joints subjected to lateral force. J Wood Sci 61:221–229
19. Awaludin A, Hirai T, Hayashikawa T, Leijten AJM (2012) A finite element analysis of bearing resistance of timber loaded through a steel plate. Civ Eng Dimens 14(1):1–6
20. Fukuoka T, Kageyama K, Kusafuka H, Hirao M (2018) New bolt tightening method with high accuracy utilizing real-time measurement of nut factor (in Japanese). Mar Eng 53(4):124–129
21. JIS B1083–2008 (2008) General rules for tightening of threaded fasteners (in Japanese). J. Standard Association, Tokyo
22. Matsubara D, Wakashima Y, Fujisawa Y, Shimizu H, Kitamori A, Ishikawa K (2018) Efects of tightening speed on torque coefficient in lag screw timber joints with steel side plates. J Wood Sci 64:112–118
23. Matsubara D, Teranishi M (2022) Evaluation of elastic stiffness in bolted timber joints for applying turn-of-nut method. J Wood Sci. https://doi.org/10.1186/s10086-022-02038-1
24. Fukuoka T (1992) Analysis of the tightening process of a bolted with a tensioner estimation by means of spring elements (in Japanese). Trans Jpn Soc Mech Eng Series A 58(549):760–764
25. Awaludin A, Smittakorn W, Hirai T (2006) Bearing properties of *Shorea obtusa* beneath a laterally loaded bolt. J Wood Sci 53:204–210
26. Matsubara D, Wakashima Y, Fujisawa Y, Shimizu H, Kitamori A, Ishikawa K (2017) Tightening torque calculation method for plastic clamp force of bolted timber joints (in Japanese). Mokuzai Gakkaishi 63(4):162–175
27. Hongo K, Yoshimoto I, Eto G, Sasaki T (1973) Investigation on the optimum tightening force of bolted joint in torque control method—experiments on the torque coefficient—(in japanese). J Jpn Soc Precision Eng 39(462):748–752
28. Hashimura S, Komatsu K, Uemura S, Matsufuji T (2010) A Study of improvement for tightening accuracy of bolted joint using lubricants (in Japanese). Des Eng 45(10):498–505

Publisher's Note